Leucine 332 at the Boundary Between the Fourth Transmembrane Segment and the Cytoplasmic Domain of Na^+,K^+-ATPase Plays a Pivotal Role in the Ion Translocating Conformational Changes†

Bente Vilsen*

Department of Physiology, University of Aarhus, DK-8000 Aarhus C, Denmark

Received May 2, 1997; Revised Manuscript Received July 22, 1997⊗

ABSTRACT: Mutants Gly330→Ala, Leu332→Ala, Leu332→Pro, and Pro780→Ala of the α_1-isoform of rat kidney Na^+,K^+-ATPase were expressed in COS-1 cells to active site concentrations between 20 and 70 pmol per mg of membrane protein. The functional properties of the mutants were characterized by titrations of Na^+-, K^+-, and ATP-dependencies of Na^+,K^+-ATPase activity as well as by a series of assays measuring the K^+-dependence of the steady-state phosphoenzyme level, the kinetics of dephosphorylation under a variety of conditions, and the ADP−ATP exchange activity. In mutants Gly330→Ala, Leu332→Ala, and Leu332→Pro, the molecular turnover number was reduced relative to that of the wild-type Na^+,K^+-ATPase, and the steady-state phosphoenzyme level was high even in the presence of several millimolar K^+. At a low Na^+ concentration in the absence of K^+, mutants Leu332→Pro and Gly330→Ala displayed high ADP−ATP exchange activity and formed a high level of the ADP-sensitive phosphoenzyme (E1P). The phosphoenzyme decayed slowly following a jump in salt concentration and chase with ATP and K^+. Hence, the conversion of E1P to the K^+-sensitive phosphoenzyme (E2P) was inhibited in mutants Leu332→Pro and Gly330→Ala. In the Leu332→Ala mutant, a high level of E2P was accumulated in the absence of K^+, and the ADP−ATP exchange activity was low at low Na^+ concentration in the absence of K^+, but rose sharply on addition of K^+. Dephosphorylation experiments indicated that in the Leu332→Ala mutant K^+ induced reversal of the phosphoenzyme interconversion, forming E1P from E2P. Leu332 is therefore a pivotal residue in the conformational change. Mutants Gly330→Ala and Pro780→Ala displayed reduced K^+ affinities relative to the wild type, determined in three independent assays.

The Na^+,K^+-ATPase[1] of animal cell membranes is an integral membrane protein responsible for the active transport of sodium and potassium ions against their electrochemical gradients (*1*). The polypeptide chain of the catalytic α-subunit of Na^+,K^+-ATPase is folded to form a large cytoplasmic domain anchored to the membrane through a number of transmembrane segments. The catalytic ATP hydrolysis site resides in the cytoplasmic part, whereas residues of importance for cation binding and selectivity have been identified in the transmembrane sequences (*2*−*6*). The coupling of ATP hydrolysis to ion translocation has classically been discussed in terms of the Albers−Post model (*1, 7, 8*), in which the Na^+,K^+-ATPase undergoes consecutive conformational changes associated with the hydrolysis of ATP and the binding and release of ions. Like other so-called "P-type ATPases", the Na^+,K^+-ATPase receives the γ-phosphoryl group from ATP at an aspartic acid residue in the catalytic site, thereby forming an acid-stable phosphorylated intermediate. The phosphoryl transfer requires triggering by sodium ions bound from the cytoplasmic side of the membrane, whereas the dephosphorylation occurring later in the enzyme cycle is activated by extracellular potassium ions. A central event in the translocation of sodium ions is the transformation of the ADP-sensitive and K^+-insensitive phosphoenzyme (E1P) to an ADP-insensitive and K^+-sensitive E2P form, which seems to involve conformational changes rearranging the catalytic site as well as the cation binding structure, thereby exposing the ion binding sites to the external side of the membrane (*1, 7, 8*). Little is known about the nature of these conformational changes and the location in the protein structure of the amino acid residues that mediate the long-range linkage between the cytoplasmic domain and the transmembrane segments. The rate of the E1P to E2P transition can be slowed down by pretreating the Na^+,K^+-ATPase with the sulfhydryl reagent *N*-ethylmaleimide (*7, 9, 10*) and by selective tryptic (*11*) or chymotryptic (*12*) cleavage of peptide bonds in the cytoplasmic domains. Certain covalently attached probes such as iodoacetamidofluorescein (bound in the cytoplasmic domain) (*13*) and benzimidazolylphenyl maleimide (bound in the putative ninth transmembrane segment M9) report on conformational changes of the phosphoenzyme. Studies of enzyme preparations doubly labeled with fluorescent probes in the cytoplasmic domain and the membrane domain suggest that the conformational changes are transmitted between these domains in a sequential rather than a concerted manner (*14*).

A likely mediator of signal transmission between the catalytic site and the cation binding sites in the transmembrane domain is the peptide segment intervening between

† This research was supported by grants from the Danish Biotechnology Program, the Danish Medical Research Council, the NOVO Nordisk Foundation, and the Research Foundation of Aarhus University.

* Correspondence address: Department of Physiology, University of Aarhus, Ole Worms Allé 160, DK-8000 Aarhus C, Denmark. FAX: +45 86 12 90 65. E-mail: bv@fi.aau.dk.

⊗ Abstract published in *Advance ACS Abstracts,* October 1, 1997.

[1] Abbreviations: E1P, ADP-sensitive and K^+-insensitive phosphoenzyme intermediate; E2P, K^+-sensitive and ADP-insensitive phosphoenzyme intermediate; $K_{0.5}$, concentration giving half-maximal effect; M1−M10, putative transmembrane segments numbered from the NH_2-terminal end of the peptide; Na^+,K^+-ATPase, sodium plus potassium-activated adenosine triphosphatase (EC 3.6.1.3).

S0006-2960(97)01030-1 CCC: $14.00

the phosphorylated aspartic acid residue and the highly conserved PEGL motif present at the cytoplasmic end of the fourth transmembrane segment M4 in the Na^+,K^+-ATPase and in other closely related P-type ATPases (*15*−*18*). Previously, it was demonstrated that the proline Pro328 and the glutamic acid residue Glu329 of the PEGL motif are involved in optimization of the Na^+ and K^+ affinities in the Na^+,K^+-ATPase (*19*−*21*), and Glu329 seems to be part of a gate at the cytoplasmic entrance to the cation binding pocket (*3, 22*). Replacement of Leu332 next to the PEGL motif with alanine led to an increase in the apparent affinities for Na^+ and ATP, suggesting a possible role for Leu332 in controlling conformational changes of the enzyme (*19*).

On the basis of these findings, as well as the results of related mutagenesis work on the sarcoplasmic reticulum Ca^{2+}-ATPase (*15, 16, 18, 23*), the present investigation was carried out to elucidate the functional roles of the residues Leu332 and Gly330 in the Na^+,K^+-ATPase. In addition to substituting either of these two residues with alanine, the leucine was also substituted with proline, the residue present at the equivalent position in the sarcoplasmic reticulum Ca^{2+}-ATPase. Furthermore, for comparison the proline Pro780 in transmembrane segment M5 was replaced with alanine. Like Gly330, this proline is located adjacent to a glutamic acid residue (Glu781) implicated in cation binding (*2, 4*), and the residue at the corresponding position in the sarcoplasmic reticulum Ca^{2+}-ATPase is a glycine, which like proline may confer conformational flexibility to the peptide segment.

To study the effects of these mutations on the E1P to E2P transition, the kinetics of dephosphorylation and the ADP−ATP exchange activity were measured under a variety of conditions. This was made feasible by the relatively high expression levels obtained using the COS cell expression system. The results of the functional analysis demonstrate that the E1P to E2P interconversion is profoundly affected by mutations to Gly330 and Leu332, and, interestingly, the Leu332→Pro mutation inhibits the transition in the forward direction, whereas the Leu332→Ala mutation seems to enhance the backward transition. The Pro780→Ala mutation in transmembrane segment M5 affects predominantly the K^+ affinity.

MATERIALS AND METHODS

Construction of the Mutant cDNAs and Expression in COS-1 Cells

Oligonucleotide-directed site-specific mutagenesis of the cDNA encoding the ouabain-resistant rat α_1-isoform of the Na^+,K^+-ATPase α-subunit was carried out according to Kunkel (*24*) essentially as described previously for mutant Leu332→Ala (*19*). Mutations corresponding to the amino acid substitutions Gly330→Ala, Leu332→Pro, and Pro780→Ala were introduced into appropriate restriction fragments (approximately 600 bp in size). The mutant cDNA fragments were sequenced throughout using the dideoxynucleotide chain termination method (*25*) and subsequently ligated with the remainder of the cDNA encoding the rat α_1-isoform of the Na^+,K^+-ATPase α-subunit to construct full-length mutated Na^+,K^+-ATPase cDNAs contained within the Bluescript vector (Stratagene, La Jolla, CA). The mutant cDNAs were then transferred to the expression vector pMT2 containing the adenovirus major late promoter (*26*) and subsequently transfected into COS-1 cells (*27*) by the calcium phosphate procedure. Cell lines carrying the respective Na^+,K^+-ATPase cDNAs stably integrated in the chromosomes were selected by inclusion of 5 μM ouabain in the growth medium to inhibit the ouabain-sensitive endogenous COS-1 cell Na^+,K^+-ATPase, and subsequently expanded into stable cell lines maintained in ouabain as described previously (*19, 20*). In order to up-regulate the expression levels of the exogenous expressed mutant and wild-type Na^+,K^+-pumps, the selection pressure was further increased by growing the COS-1 cells at limiting K^+ concentrations of 2 mM or less (*4*).

Plasma Membrane Preparations and Assay for Na^+,K^+-ATPase Activity

A crude plasma membrane fraction from the COS-1 cells was isolated and the vesicles made leaky by incubation with deoxycholate (*19, 20*). Total protein concentration was determined by the dye binding method of Bradford (*28*) using bovine serum albumin as standard. The ATPase activity of the wild type or mutants at various concentrations of Na^+, K^+, and ATP (added as Tris salt) was measured on leaky membrane vesicles at 37 °C by determination of inorganic phosphate liberation as previously (*19, 20*). In all titrations of Na^+,K^+-ATPase activity, at least three separate membrane preparations corresponding to different clonal isolates of cells transfected with the same cDNA were assayed in duplicate. There were no significant differences between the $K_{0.5}$ values for Na^+, K^+, and ATP obtained with the different clonal isolates.

Na^+ Dependent ADP−ATP Exchange Activity

ADP−ATP exchange activity was measured by the formation of [^{14}C]ATP during incubation of the leaky membrane preparation (12 μg of total membrane protein) at 26 °C with unlabeled ATP (5 mM) and [^{14}C]ADP (1.25 mM) in a 100 μL volume containing 0.15 mM $MgCl_2$, 1 mM EGTA, 20 mM Tris buffer (pH 7.5), various concentrations of NaCl, KCl, and choline chloride (to keep the ionic strength constant), and 10 μM or 7.25 mM ouabain. The membrane suspension was preincubated in the absence of Na^+ for 30 min at room temperature, with either 10 μM ouabain to inhibit the endogenous COS-1 cell Na^+,K^+-ATPase or with 7.25 mM ouabain to inhibit in addition the exogenous wild-type and mutant rat Na^+,K^+-ATPases (*29*). The ADP−ATP exchange activity contributed by the expressed wild-type or mutant rat kidney Na^+,K^+-ATPase was then calculated as the difference between the respective activities determined at 10 μM and 7.25 mM ouabain. The ADP−ATP exchange activity was constant over an incubation period of 15−90 min. A Mg^{2+} concentration as low as 0.15 mM was chosen because preliminary studies of the dependence of the ADP−ATP exchange activity on Mg^{2+} showed that high Mg^{2+} concentrations were inhibitory, possibly because free ADP rather than MgADP is the substrate (*9*). Moreover, at the low Mg^{2+} concentration the background of Mg^{2+}-activated nucleotide exchange unrelated to the Na^+-activated ADP−ATP exchange activity of Na^+,K^+-ATPase was considerably reduced (cf. also (*29*)). The ADP−ATP exchange reaction was terminated by placing the vials in boiling water for 2 min. To separate ATP, ADP, and AMP, 40 μL of reaction

mixture was applied to a cellulose MN 300 polyethyleneimine impregnated thin-layer chromatographic plate (*30*) along with nucleotide standards, and chromatography carried out in the presence of 0.85 M KH_2PO_4 (pH 3.4). The nucleotide spots that were visualized under ultraviolet light (254 nm) were cut out and eluted in 3 mL of 0.7 M $MgCl_2$, 20 mM Tris-HCl, and the radioactivity contained in the spots was quantitated by liquid scintillation counting.

Phosphoenzyme Formation and Decay

Phosphorylation of the leaky membrane suspension (10 μg total membrane protein) was carried out for 10 s at 0 °C in 100 μL of standard medium containing 2 μM [γ-^{32}P]ATP, 20 mM Tris (pH 7.4), 3 mM $MgCl_2$, 1 mM EGTA, 10 μM ouabain, and various concentrations of NaCl and KCl (indicated in the figure legends) and choline chloride to keep the ionic strength constant (total concentration [KCl] + [NaCl] + [choline chloride] = 150 mM except in the experiments reported in Figure 3). In the absence of added KCl, the complete reaction mixture contained less than 10 μM K^+ (usually around 5 μM) as measured by flame photometry. Experiments with higher ATP concentrations indicated that 2 μM ATP was sufficient to obtain >90% saturation of phosphorylation in the absence of added KCl. To verify that the steady-state phosphorylation level was reached within the 10 s, longer incubation times (up to 60 s) were routinely tried.

Acid quenching for determination of the amount of phosphorylated Na^+,K^+-ATPase protein was performed either directly after the phosphorylation period or at serial time intervals following the addition of a chase solution to monitor the dephosphorylation rate. During phosphorylation and dephosphorylation, the reaction mixture was stirred continually by a vertically orientated tiny magnet bar (8 mm × 1 mm) contained in an Eppendorf tube immersed in ice−water (0 °C), and the ice-cold chase and quench solutions were added manually, timing being controlled by an electronic metronome.

The background phosphorylation was determined in the presence of 50 mM KCl without NaCl. In the kinetic experiments and in titrations of ligand concentration dependence of steady-state phosphorylation, where it was essential to minimize background phosphorylation, the acid-quenched denatured and precipitated protein was washed by centrifugation and subjected to acid SDS-polyacrylamide gel electrophoresis (*15*). The quench and wash solutions consisted of 1 and 0.25 M phosphoric acid (titrated to pH 2.4 with NaOH), respectively. The radioactivity associated with the protein band that migrated to approximately 100 kDa on the gel was quantitated by electronic autoradiography using a Packard InstantImager apparatus. Representative examples of the appearance of this band on autoradiographs are shown in Figure 3. No other distinct radioactive bands were detectable on the autoradiographs (only a faint smear corresponding to much lower molecular size), and the background phosphorylation measured at the 100-kDa position following phosphorylation in the presence of 50 mM KCl without NaCl (last lane in the examples shown in Figure 3) was always less than 10% of the maximum phosphorylation.

For determination of the absolute value for the maximum phosphorylation level ("active site concentration") used in the calculation of turnover number, the leaky membrane suspension was preincubated for 10 min at 20 °C with 20 μg of oligomycin/mL to stabilize the phosphoenzyme (*4*) and the phosphorylation was carried out in the presence of 150 mM Na^+ without added KCl. A filtration technique replaced the centrifugal washing and acid SDS−polyacrylamide gel electrophoresis of the acid-quenched protein. Acid quenching was performed with 7% trichloroacetic acid containing 2 mM pyrophosphate and 1.2 mM ATP. The precipitate was collected on glass fiber filter discs (GC 50, Advantec Toyo) and washed four times with 4 mL of 5% trichloroacetic acid containing 2 mM pyrophosphate and 0.6 mM ATP. The filtration technique was not generally used in the present study, because the background, comprising as much as 20−40% of the maximum amount of phosphoenzyme, was considered too large for accurate determination of the submaximal phosphorylation levels in the kinetic and ligand titration experiments.

Unless otherwise indicated, the phosphorylation levels presented in the figures are average values (corrected for background phosphorylation) corresponding to at least two independent experiments each performed in duplicate. Standard errors (not shown in the figures) were generally lower than 5% and did never exceed 10%. Data obtained in kinetic experiments (Figures 2−7) are presented as the percentage of the initial phosphoenzyme level determined at the time of addition of the chase solution.

Purification of the Nucleotides

[^{14}C]ADP and ATP used in nucleotide exchange and dephosphorylation experiments were purified by chromatography on a Sephadex DEAE-A25 column. ATP thus purified contained less than 0.2 mol % ADP, as measured by determining the amount of NADH being converted to NAD^+ upon mixing the ATP solution with phosphoenolpyruvate (1 mM), pyruvate kinase (10 IU/mL), lactate dehydrogenase (10 IU/mL), and NADH (0.1 mM). Control experiments showed that this assay was sensitive enough to detect 0.1 mol % ADP.

Procedures for Curve Fitting and Computer Simulation

Data were analyzed by nonlinear regression using the Sigmaplot program (Jandel Scientific). The ligand concentration dependencies of ATPase activity, phosphorylation, and initial rate of K^+-induced dephosphorylation (Table 1, Figures 4 and 5) were fitted to the modified Hill equation

$$V = (V_{max} - V_o)[L]^n/(K_{0.5}^n + [L]^n) + V_o$$

where V_{max} is the rate corresponding to infinite ligand concentration and V_o corresponds to the basic rate measured in the absence of ligand.

The phosphoenzyme decay curves shown in Figures 2−6 were obtained by fitting the data points to the sum of two exponentials:

$$\% \text{ phosphorylation} = (100\% - a)e^{-k_1 t} + ae^{-k_2 t}$$

where k_1 and k_2 represent the rate coefficients of the rapid and slow components, respectively, of the decay curves and a the extent of the slow component.

The effects on the overall enzyme turnover of varying the rate coefficients of partial reactions were evaluated by

Table 1: Apparent Affinities for ATP, Na^+, and K^+ and Turnover Numbers

mutant	ATPase activity[a] $K_{0.5}$ (mM) ATP	Na^+	K^+	EP[b] $K_{0.5}$ (μM) Na^+	turnover rate[c] (min^{-1})
wild type	0.278	7.13	0.78	692 ± 74	8474 ± 165
Gly330→Ala	0.046	3.64	3.13	141 ± 21	6796 ± 414
Leu332→Ala	0.042	3.92	1.97	447 ± 24	4309 ± 264
Leu332→Pro	0.035	3.48	1.00	466 ± 37	5452 ± 291
Pro780→Ala	0.100	6.77	3.50	660 ± 54	9028 ± 351

[a] The Na^+,K^+-ATPase measurements were carried out at 37 °C, pH 7.4, in the presence of 3 mM $MgCl_2$, 1 mM EGTA, 10 μM ouabain, and varying concentrations of Na^+, K^+, and ATP. The ionic strength was kept constant by addition of choline chloride (total concentration [KCl] + [NaCl] + [choline chloride] = 150 mM). For determination of $K_{0.5}(Na^+)$ the K^+ and ATP concentrations were 20 and 3 mM, respectively, and the Na^+ concentration was varied between 1 and 130 mM. For determination of $K_{0.5}(K^+)$ the Na^+ and ATP concentrations were 40 and 3 mM, respectively, and the K^+ concentration was varied between 0.25 and 30 mM. For determination of $K_{0.5}$(ATP) the Na^+ and K^+ concentrations were 130 and 20 mM, respectively, and the ATP concentration was varied between 10 μM and 5 mM. For each ligand concentration the measurement was repeated at least six times and average values, corrected for background ATPase activity measured in presence of 10 mM ouabain, were fitted to the Hill equation as described under Materials and Methods. [b] Phosphorylation was carried out at 0 °C in standard medium containing varying concentrations of Na^+ in the presence of oligomycin and without added KCl. Phosphorylation data points corresponding to each independent series of experiments were fitted to the Hill equation. Mean of the $K_{0.5}$ values ± SEM (n = 3−4) is indicated. [c] The turnover rate was calculated as the ratio between the maximum Na^+,K^+-ATPase activity, measured at 37 °C in the presence of saturating Na^+, K^+, and ATP concentrations, and the active site concentration determined in phosphorylation experiments in the presence of 150 mM Na^+ and oligomycin (20 μg/mL) without added KCl using the filtration method described under Materials and Methods. Mean ± SEM of 5−11 experiments is indicated.

computation using the NEWSIM2 simulation program kindly provided by Dr. G. Inesi (*31*).

RESULTS

Expression and Ouabain Sensitivity

The expression strategy takes advantage of the well-established 500-fold difference between the ouabain sensitivities of the rat kidney Na^+,K^+-ATPase and the endogenous COS cell Na^+,K^+-ATPase, which because of the preferential inhibition of the endogenous enzyme in the presence of ouabain allows selection of transfected cells expressing functional exogenous enzyme (*20*).

In addition to the wild-type rat kidney Na^+,K^+-ATPase, the mutants Gly330→Ala, Leu332→Ala, Leu332→Pro, and Pro780→Ala were all found to be able to confer ouabain resistance to the COS cells, demonstrating the ability of these mutant enzymes to transport Na^+ and K^+ at rates sufficiently high to support cell growth.

When the effect on the Na^+,K^+-ATPase activity of variation of the ouabain concentration was examined on plasma membranes isolated from the stable COS cell lines expressing exogenous wild-type Na^+,K^+-ATPase or mutants, it was found that each of the mutants, like the wild type, showed a monophasic response to ouabain with an apparent affinity for ouabain about 500-fold lower than that of the ouabain-sensitive endogenous COS cell Na^+,K^+-ATPase (not shown). Therefore, the ouabain binding properties were not significantly affected by the substitution of the residues Gly330, Leu332, and Pro780, although Pro780 is located in relatively close proximity to the M5−M6 extracellular loop recently implicated in ouabain binding (*32*). Hence, it can be excluded that the functional differences to be described below, between the wild type and the mutants Gly330→Ala, Leu332→Ala, Leu332→Pro, and Pro780→Ala, were caused by differences in ouabain sensitivity.

Na^+, K^+, and ATP Dependencies of Na^+,K^+-ATPase Activities

Table 1 summarizes the results of experiments in which the Na^+,K^+-ATPase activity was determined at various Na^+, K^+, and ATP concentrations on membranes containing expressed ouabain-resistant rat Na^+,K^+-ATPase corresponding to either wild type or the mutants Gly330→Ala, Leu332→Ala, Leu332→Pro, and Pro780→Ala. The corresponding titration curves have been previously published for the wild type and mutant Leu332→Ala (*19*). The Na^+,K^+-ATPase activity measurements were performed in the presence of 10 μM ouabain, because this concentration of ouabain preferentially inhibits the endogenous ouabain-sensitive COS cell Na^+,K^+-ATPase. As previously demonstrated, the activity contributed by the endogenous enzyme constituted less than 5% of the total activity under these assay conditions (*19*).

The Pro780→Ala mutant displayed a $K_{0.5}$ for Na^+ very similar to that of the wild-type enzyme, whereas each of the mutants Gly330→Ala, Leu332→Ala, and Leu332→Pro exhibited a slight (2-fold) increment of apparent affinity for Na^+. The K^+ titrations of ATPase activity showed that the mutants Leu332→Ala and Leu332→Pro only displayed slightly reduced apparent affinities for K^+. The mutants Gly330→Ala and Pro780→Ala, on the other hand, exhibited $K_{0.5}$ values corresponding to a 4−5-fold reduction of apparent affinity for K^+ relative to the wild-type enzyme.

Titration of the ATP concentration dependence of Na^+,K^+-ATPase activity of mutants Gly330→Ala, Leu332→Ala, and Leu332→Pro provided $K_{0.5}$ values for ATP corresponding to an increment in apparent affinity of 6−8-fold relative to the wild type. For the mutant Pro780→Ala, only a 2.8-fold increase in the apparent affinity for ATP was observed. Because the activation of the enzyme by ATP studied here reflects predominantly the binding of ATP to a low-affinity site on the E2 form of the dephosphoenzyme, whereas the catalytic site in the E1 form exhibits high affinity for ATP, the observed effects of the mutations on the apparent ATP affinity may result from a shift of the E2−E1 equilibrium in favor of E1 (cf. (*20*)).

Na^+ Dependence of Steady State Phosphorylation

Because the apparent Na^+ affinity measured by titration of Na^+,K^+-ATPase activity (see above) is affected by the competition between K^+ and Na^+ at the cation-binding sites, it was furthermore desirable to determine the apparent Na^+ affinity in the absence of K^+. This was accomplished by measuring the steady-state phosphoenzyme level formed from ATP at varying Na^+ concentrations. From the results summarized in Table 1, it can be seen that there was a general reduction in the $K_{0.5}$ values relative to those obtained in the Na^+,K^+-ATPase assay. The mutants Leu332→Ala and Leu332→Pro exhibited a 1.5-fold increase in the apparent

Na^+ affinity relative to the wild-type Na^+,K^+-ATPase, whereas for mutant Gly330→Ala the increase amounted to as much as 5-fold, and the Na^+ affinity displayed by the mutant Pro780→Ala was almost identical to that of the wild type.

Site Concentrations and Maximum Molecular Activity (Turnover Number)

The active site concentration was determined by measuring the maximum steady-state phosphoenzyme level using the filtration method (see Materials and Methods). Expression levels of the wild type and the Pro780→Ala mutant ranged betweeen 20 and 50 pmol active sites per mg of total membrane protein, whereas the mutants Gly330→Ala, Leu332→Ala, and Leu332→Pro generally were expressed to somewhat higher levels, reaching 70 pmol per mg of total membrane protein.

The determination of the active site concentration allowed calculation of the maximum molecular activity (turnover number) from the maximum ATPase activity measured in the presence of saturating Na^+, K^+, and ATP concentrations (Table 1). The exogenous rat wild-type Na^+,K^+-ATPase displayed a turnover number of approximately 8500 min^{-1}, in good agreement with the turnover numbers of purified Na^+,K^+-ATPase from various species (*33*). Previously, a somewhat higher value was reported for the rat wild-type Na^+,K^+-ATPase expressed in COS cells, using the acid gel electrophoretic procedure for determination of the phosphorylation (*4, 20*). The latter procedure results in an underestimation of the absolute phosphoenzyme level due to loss of a certain fraction of the phosphorylated protein during centrifugal washing and gel electrophoresis.

As seen in Table 1, the mutants Gly330→Ala, Leu332→Ala, and Leu332→Pro displayed significantly reduced Na^+,K^+-ATPase turnover numbers relative to the wild type, whereas the turnover number of the Pro780→Ala mutant was similar to or tended to be slightly increased relative to that of the wild-type Na^+,K^+-ATPase.

K^+ Dependence of Steady-State Phosphoenzyme Formed from ATP

The effect of K^+ on the steady-state level of phosphoenzyme formed from ATP at 20 mM Na^+ was examined over a wide range of K^+ concentrations at 0 °C (Figure 1). Both the wild-type Na^+,K^+-ATPase and the Pro780→Ala mutant exhibited a strong response to K^+ in the submillimolar concentration range with the steady-state phosphoenzyme concentration being reduced to a plateau level of approximately 20% at saturating K^+ concentrations. Half-maximum reduction of the phosphoenzyme level of the wild-type Na^+,K^+-ATPase was obtained at approximately 85 μM K^+, in good agreement with the previous determination of an apparent K_d for K^+ of 80 μM in analogous measurements on guinea pig kidney enzyme (*34*). The titration curve for the Pro780→Ala mutant was displaced toward higher K^+ concentrations with half-maximum reduction of the phosphoenzyme level being obtained at approximately 450 μM K^+. The 5-fold difference between the apparent K^+ affinities of mutant Pro780→Ala and the wild type is in good agreement with the above described difference determined by titration of the Na^+,K^+-ATPase activity.

By contrast, the mutants Leu332→Ala and Leu332→Pro displayed high steady-state plateau levels of phosphoenzyme

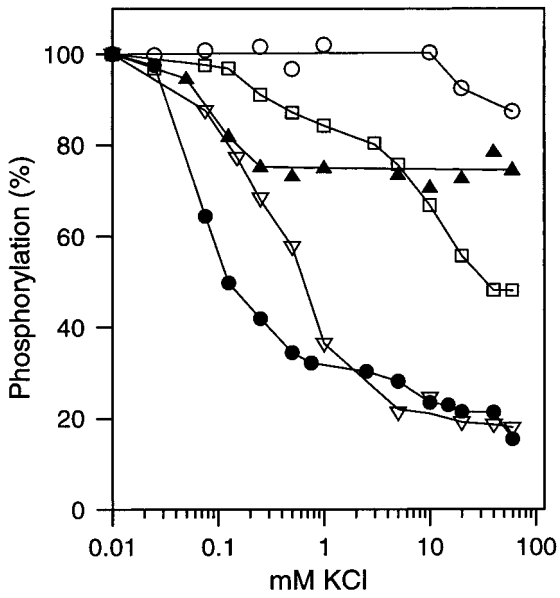

FIGURE 1: K^+-dependence of steady-state phosphorylation from ATP in the wild-type Na^+,K^+-ATPase (●) and mutants Gly330→Ala (□), Leu332→Pro (○), Leu332→Ala (▲), and Pro780→Ala (▽). Phosphorylation was carried out in standard medium containing 20 mM NaCl and various KCl concentrations as indicated. The acid-quenched samples were subjected to SDS−polyacrylamide gel electrophoresis at pH 6.0. The average values resulting from three independent experiments each in duplicate are presented as the percentage of the steady-state phosphoenzyme level obtained in the absence of KCl. The filtration procedure, described under Materials and Methods, was also tried, and there was no significant difference between the relative phosphorylation levels obtained by the two different methods.

in the presence of high K^+ concentrations in the millimolar range. The Leu332→Pro mutant did not respond at all to micromolar K^+, and close to 90% of the enzyme sites remained phosphorylated in the presence of 60 mM K^+. The steady-state phosphoenzyme level of the Leu332→Ala mutant was reduced to approximately 75% with half-maximum effect being attained at approximately 90 μM K^+ (i.e., a value almost identical to that pertaining to the wild type), but no further reduction was observed.

The Gly330→Ala mutant responded to varying K^+ concentrations in a complex manner. As seen in Figure 1, the phosphoenzyme profile of this mutant as a function of K^+ concentration is biphasic. First, there is a decrease to a plateau level of approximately 80% with half-maximum effect being attained at approximately 300 μM K^+, followed by another decrease to a plateau level of 50% with half-maximum effect at approximately 10 mM K^+. Thus, the results obtained with the Gly330→Ala mutant reveal a high-affinity component as well as a low-affinity component.

Similar phosphorylation experiments carried out at 26 °C demonstrated that also at this temperature the Leu332→Ala, Leu332→Pro, and Gly330→Ala mutants displayed a higher phosphorylation level than the wild type in the presence of millimolar K^+ concentrations (data not shown).

The experiments described below were designed to further investigate the extraordinary properties of the phosphoenzymes formed by these mutants.

ADP Dependent Dephosphorylation Kinetics at 130 and 2 mM Na^+

Two main types of phosphoenzyme intermediates are classically distinguished in the wild-type Na^+,K^+-ATPase

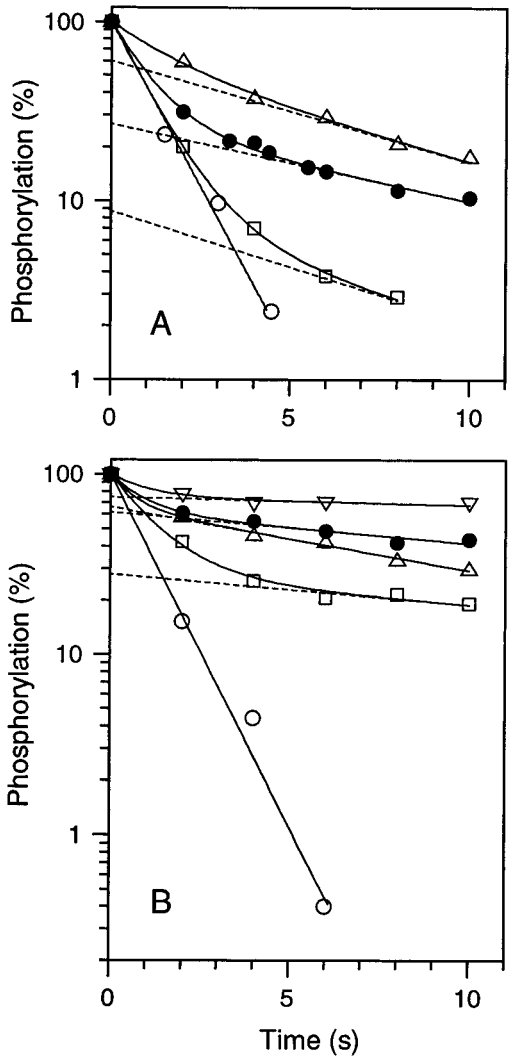

FIGURE 2: Time courses of ADP-dependent dephosphorylation of phosphoenzyme formed by the wild-type Na^+,K^+-ATPase and mutants Gly330→Ala, Leu332→Pro, Leu332→Ala (both panels), and Pro780→Ala (only in panel B). Phosphorylation was carried out in 100 μL standard medium in the absence of added KCl and presence of 130 mM NaCl (A) or 2 mM NaCl (B). This was followed by addition of 10 μL of chase solution (corresponding to zero time) producing final concentrations of 2.5 mM ADP and 1 mM unlabeled ATP, and dephosphorylation was terminated by acid quenching at the indicated serial times. The data were fitted to biexponential decay curves as described under Materials and Methods. The respective values for the extent of the slow component of the decay curve and the rate coefficients of the fast and slow components were the following: (A) wild type (●), 27%, 1.0 and 0.1 s^{-1}; mutant Gly330→Ala (□), 9%, 0.96 and 0.14 s^{-1}; mutant Leu332→Pro (○), 100%, 0.85 s^{-1} (single exponential); mutant Leu332→Ala (△), 60%, 0.62 and 0.13 s^{-1}; (B) wild type (●), 62%, 1.1 and 0.04 s^{-1}; mutant Gly330→Ala (□), 28%, 0.8 and 0.04 s^{-1}; mutant Leu332→Pro (○), 100%, 0.9 s^{-1} (single exponential); mutant Leu332→Ala (△), 66%, 1.5 and 0.08 s^{-1}; mutant Pro780→Ala (▽), 75%, 0.92 and 0.01 s^{-1}. Dashed lines show extrapolation of the slow decay component back to ordinate intercept.

by their different reactivities toward ADP and K^+. E1P is ADP sensitive, i.e., able to donate the phosphoryl group back to ADP forming ATP, but resistant to K^+. E2P is resistant to ADP but sensitive to K^+, i.e., dephosphorylates in the presence of K^+. In addition to E1P and E2P, intermediate phosphoenzyme forms sensitive to both ADP and K^+ have been described. The proportion of the phosphoenzyme accumulated in the ADP-sensitive form at steady state increases with increasing Na^+ concentration, whereas the proportion of ADP-insensitive phosphoenzyme decreases (*35*−*37*).

Table 2: Na^+ and K^+ Dependencies of ADP−ATP Exchange Activity

	molecular ADP−ATP exchange activity (min^{-1})[a]			
mutant	20 mM Na^+	20 mM Na^+ 20 mM K^+	130 mM Na^+ 20 mM K^+	200 mM Na^+
wild type	0[b]	2 ± 10	30 ± 10	92 ± 19
Gly330→Ala	127 ± 25	ND[c]	178 ± 28	ND
Leu332→Pro	114 ± 7	192 ± 51	200 ± 23	ND
Leu332→Ala	0[b]	94 ± 10	187 ± 19	ND

[a] The molecular ADP−ATP exchange activity was calculated as the ratio between the ADP−ATP exchange activity determined as described under Materials and Methods and the active site concentration determined by the phosphorylation method. Mean ± SEM of 4−18 experiments is indicated. [b] No detectable ADP−ATP exchange activity. [c] Not determined.

Figure 2 shows results of two series of experiments in which the kinetics of ADP-dependent dephosphorylation were studied following phosphorylation either at 130 mM Na^+ (Figure 2A) or at 2 mM Na^+ (Figure 2B).

In mutant Leu332→Pro, addition of ADP in the absence of K^+ produced a fast monophasic decay of the phosphoenzyme irrespective of whether phosphorylation had been carried out in the presence of 130 mM Na^+ or 2 mM Na^+. This indicates that under both conditions the accumulated phosphoenzyme resided almost exclusively in the ADP-sensitive form. For each of the other mutants and the wild-type Na^+,K^+-ATPase, the time course of ADP-induced dephosphorylation consisted of more than one exponential decay component at both Na^+ concentrations. Fitting of the data to the sum of two exponentials provides a minimum estimate of the amount of ADP-insensitive E2P present from extrapolating the slow decay phase back to ordinate intercept (dashed lines). From Figure 2A, it appears that the fraction of phosphoenzyme sensitive to ADP decreases in the order Gly330→Ala > wild type > Leu332→Ala, but the exact amount of E1P is difficult to estimate due to insufficient separation of the components of the decay curves, which actually may consist of three or more components (*35*, *38*). At the lower Na^+ concentration (Figure 2B), the rapid decay component was more clearly separated from the remaining part of the curve. In the wild type and mutants Leu332→Ala and Pro780→Ala a high level of E2P was found to accumulate corresponding to ordinate intercepts at 62%, 66%, and 75%, respectively. The phosphoenzyme formed by the Gly330→Ala mutant like that of the Leu332→Pro mutant was predominantly ADP-sensitive E1P (28% E2P from ordinate intercept).

ADP−ATP Exchange Activity at 26 °C

To examine the partition of the phosphoenzyme intermediate between ADP-sensitive and ADP-insensitive forms under steady-state conditions at higher temperatures as well, the ADP−ATP exchange activity was determined by measurement of formation of radioactive ATP from ^{14}C-labeled ADP (Table 2). At 20 mM Na^+, no ADP−ATP exchange activity was detectable with the wild-type enzyme, presumably because the major phosphoenzyme intermediate accumulated at steady state under these conditions is the ADP-insensitive E2P form. By contrast, the Leu332→Pro mutant as well as

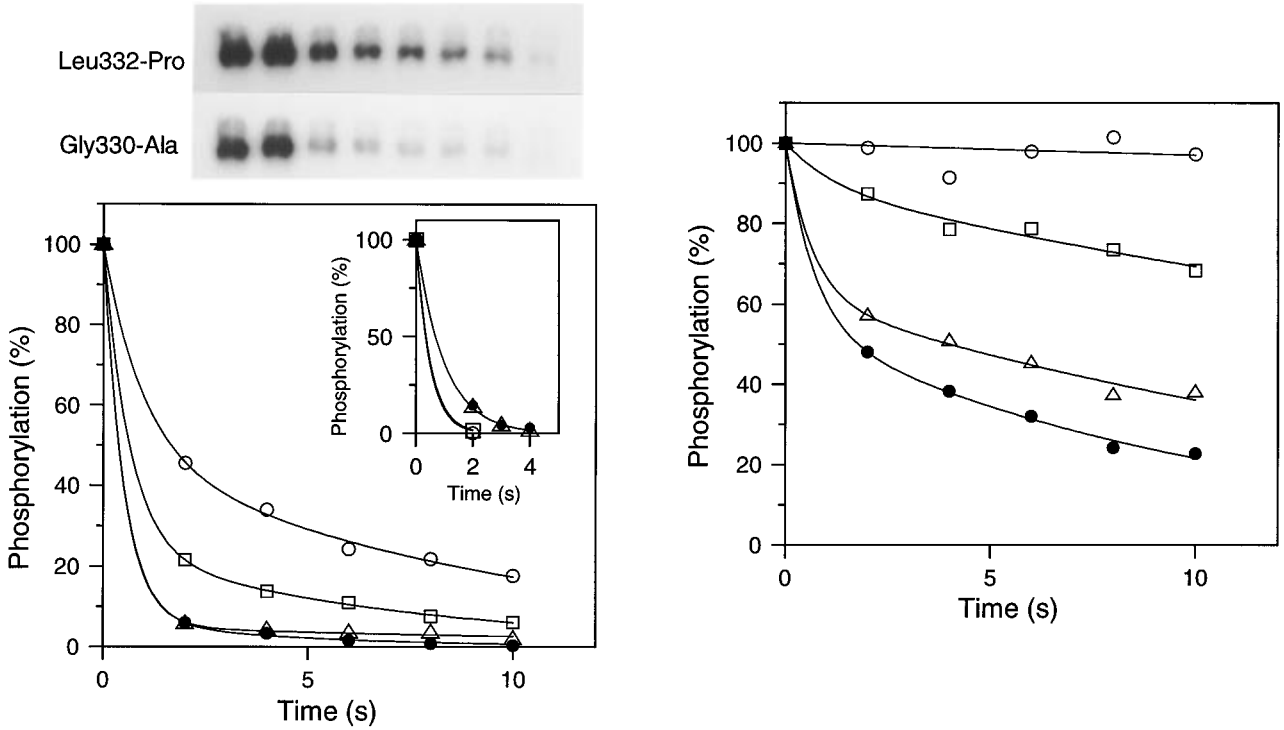

FIGURE 3: Dephosphorylation of phosphoenzyme formed at 600 mM NaCl in the wild-type Na^+,K^+-ATPase and the mutants Gly330→Ala, Leu332→Pro, and Leu332→Ala, following (left panel, main part) dilution of NaCl to 100 mM (inducing E1P to E2P interconversion) with simultaneous addition of 20 mM KCl and 1 mM unlabeled ATP, or (right panel) dilution with medium containing the same NaCl concentration as initially present (600 mM) with simultaneous addition of 20 mM KCl and 1 mM unlabeled ATP, or (inset) addition of 2.5 mM ADP with 1 mM unlabeled ATP without dilution of the 600 mM NaCl. Phosphorylation was carried out in 100 μL of standard medium in the presence of 600 mM NaCl and absence of added KCl and terminated (corresponding to zero time) by addition of 500 μL (left panel, main part and right panel) or 10 μL (inset) of chase solution. In addition to the above described components, the chase solution contained the following components of the standard phosphorylation medium: 1 mM EGTA, 3 mM $MgCl_2$, 20 mM Tris (pH 7.4). The data were fitted to biexponential decay curves as described under Materials and Methods. Note that to accomodate the inset the ordinate is not logarithmic. The respective values for the extent of the slow component of the decay curve and the rate coefficients of the fast and slow components were the following: (left panel, main part) wild type (●), 7%, 2.0 and 0.24 s^{-1}; mutant Gly330→Ala (□), 24%, 1.6 and 0.14 s^{-1}; mutant Leu332→Pro (○), 48%, 1.0 and 0.10 s^{-1}; mutant Leu332→Ala (△), 5%, 2.0 and 0.068 s^{-1}; (right panel) wild type (●), 55%, 1.4 and 0.093 s^{-1}; mutant Gly330→Ala (□), 89%, 0.84 and 0.025 s^{-1}; mutant Leu332→Pro (○), 100%, 0.003 s^{-1} (single exponential); mutant Leu332→Ala (△), 62%, 1.6 and 0.054 s^{-1}. The ADP dephosphorylation data in the inset for wild type (●), mutant Gly330→Ala (□), mutant Leu332→Pro (○), and mutant Leu332→Ala (△) were fitted to single exponentials. Shown above the left panel are representative examples of autoradiographs of the 100 kDa radioactive bands on the gels corresponding to the data in the left panel, main part for mutants Leu332→Pro and Gly330→Ala. The first seven lanes on the gel correspond to the following time points for dephosphorylation (from left to right): 0, 0, 2, 4, 6, 8, and 10 s. The last lane shows background phosphorylation.

the Gly330→Ala mutant showed high ADP−ATP exchange activities, consistent with the accumulation of the ADP-sensitive E1P phosphoenzyme at steady state. At higher Na^+ concentrations, the ADP−ATP exchange activity of the wild type increased, although values as high as those detected for the two mutants Leu332→Pro and Gly330→Ala were never reached with the wild type. The behavior of the Leu332→Ala mutant was somewhat surprising. At 20 mM Na^+ without K^+ this mutant resembled the wild-type Na^+,K^+-ATPase by showing no detectable ADP−ATP exchange activity. The addition of 20 mM K^+, however, increased the ADP−ATP exchange activity of the Leu332→Ala mutant very significantly, whereas such an effect was not observed for the wild-type Na^+,K^+-ATPase, and at 130 mM Na^+ and 20 mM K^+ the Leu332→Ala mutant exhibited ADP−ATP exchange activity of a magnitude similar to that of the mutants Leu332→Pro and Gly330→Ala.

Dephosphorylation Kinetics of Phosphoenzyme Formed at 600 mM Na^+

To compare the rates of the E1P to E2P transition of the wild type and the mutants, phosphorylation was carried out in the presence of a high Na^+ concentration of 600 mM to ensure accumulation of E1P even in the wild type (*39*). Under these conditions the phosphoenzyme formed by the wild type as well as the mutants decayed within 2−4 s following addition of ADP, indicating that it was fully ADP-sensitive (Figure 3, inset). The conversion of E1P to E2P was monitored by jumping the Na^+ concentration downward to 100 mM simultaneously with the addition of 1 mM non-radioactive ATP (to terminate phosphorylation) and 20 mM K^+ (to ensure rapid dephosphorylation of E2P). Figure 3 (left panel) shows that the dephosphorylation and thus the E1P to E2P conversion was rather fast in the wild type as well as the Leu332→Ala mutant, explaining the above described accumulation of the ADP-insensitive E2P phosphoenzyme in steady state at low Na^+ and absence of K^+. The dephosphorylation was considerably slower in the Leu332→Pro and Gly330→Ala mutants, consistent with the observed tendency for accumulation of the ADP-sensitive phosphoenzyme in steady state in these mutants. The decay curves consisted of two or more components. Such heterogenous kinetics of E1P decay has previously been described for the wild-type Na^+,K^+-ATPase and may be attributable

to heterogeneity of the lipid environment (*38, 39*). Fitting of the data to the sum of two exponentials showed that the mutations Leu332→Pro and Gly330→Ala reduced the extent of the rapid component as well as the rate coefficient of either component. The effects were more pronounced for mutation Leu332→Pro compared with mutation Gly330→Ala (for rate coefficients see the legend to Figure 3).

When similar experiments were carried out without any jump in salt concentration, i.e., with 600 mM Na^+ and 20 mM K^+ present in the dilution medium, the extent of the rapid component as well as the rate coefficient of either component were found to be reduced in the wild type as well as the mutants relative to the situation at 100 mM Na^+, and the differences between the decay curves of wild type and mutants Leu332→Pro and Gly330→Ala remained conspicuous (Figure 3, right panel). In fact, within 10 s the Leu332→Pro mutant did not dephosphorylate at all, whereas the wild-type phosphoenzyme decayed to about 20%. Under these experimental conditions, it was moreover clear that the rate coefficient of the slow decay component of the Leu332→Ala mutant is significantly lower than that of the wild type (about 2-fold).

In addition, control experiments were carried out in which phosphoenzyme formed at 130 mM Na^+ was diluted into a medium containing 130 mM Na^+, 20 mM K^+, and 1 mM ATP following the same dilution procedure as described for the results in Figure 3. Under these conditions the decay curves were found to be indistinguishable from decay curves obtained in experiments in which 20 mM K^+ and 1 mM ATP were added directly omitting the dilution step, indicating that the dilution of the protein *per se* had no significant influence on the dephosphorylation kinetics (data not shown).

K^+ Dependent Dephosphorylation Kinetics of Phosphoenzyme Formed at 2 mM Na^+

In the wild-type Na^+,K^+-ATPase, dephosphorylation of the E2P phosphoenzyme intermediate is activated by micromolar concentrations of K^+, and measurement of the dephosphorylation kinetics at varying K^+ concentrations may provide information about the interaction of K^+ with the extracytoplasmically facing uptake sites. Figures 4 and 5 show results of measurements on the wild type as well as the mutants Pro780→Ala, Leu332→Ala, and Gly330→Ala of the K^+-dependence of dephosphorylation of phosphoenzyme which had been formed at a rather low Na^+ concentration of 2 mM to promote as much as possible the accumulation of E2P (cf. Figure 2B) in addition to minimizing competition from Na^+ at the K^+ sites.

The left panels of Figures 4 and 5 show the time courses of dephosphorylation at four different K^+ concentrations of 10 mM, 1 mM, 100 μM, and 5 μM (contaminant K^+). The decay curves corresponding to K^+-induced dephosphorylation consisted of at least two components as also described above for Figure 3. Fitting of the data in Figures 4 and 5 to the sum of two exponentials showed that for the wild type as well as the mutants both rate coefficients increased with increasing K^+ concentration (for rate coefficients see legends to figures). Good fits were obtained when the extent of the slow component was kept constant at 25% independent of the K^+ concentration. The K^+ dependency of the initial dephosphorylation rate (reflecting predominantly the rapid component) is presented in the right panels of Figure 4. The

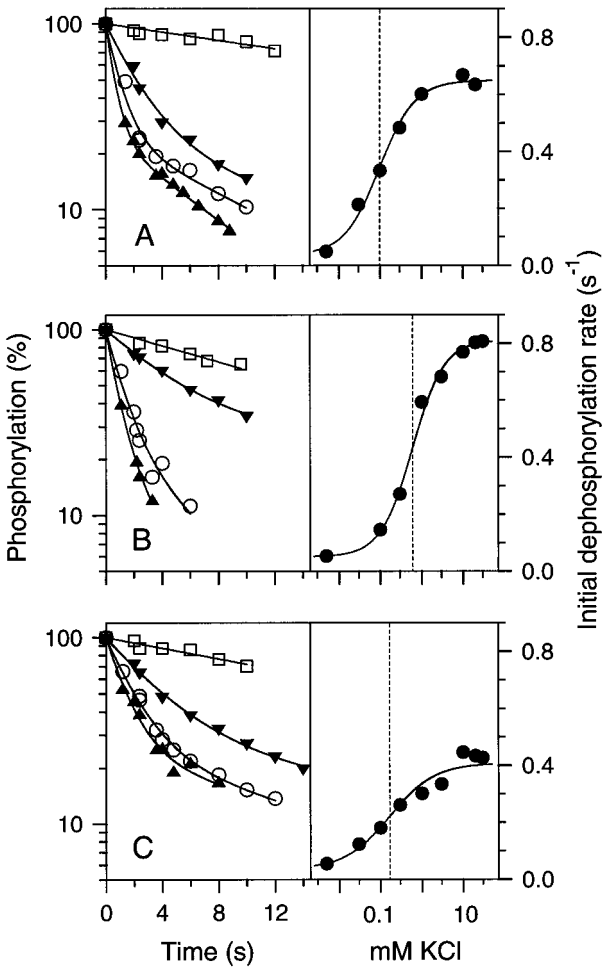

FIGURE 4: K^+-dependence of dephosphorylation of phosphoenzyme formed in presence of 2 mM NaCl in the wild-type Na^+,K^+-ATPase (A), mutant Pro780→Ala (B), and mutant Leu332→Ala (C). Left panels: Time courses of dephosphorylation at K^+-concentrations of 10 mM, 1 mM, 0.1 mM, and 5 μM (contaminant K^+). Right panels: Initial rates of dephosphorylation as a function of K^+ concentration (calculated from decays measured at 2.4 s, note the inclusion of data points corresponding to additional K^+ concentrations). Phosphorylation was carried out in 100 μL standard medium in presence of 2 mM NaCl and in the absence of added KCl and terminated (corresponding to zero time) by addition of 10 μL of a chase solution to produce 1 mM unlabeled ATP and various concentrations of KCl. Left panels: The data points were fitted to biexponential decay curves as described under Materials and Methods. The respective values for the extent of the slow component of the decay curve and the rate coefficients of the fast and slow components were the following. (A) Wild type: chase without added K^+ (□), 100%, 0.026 s^{-1} (single exponential); chase with 100 μM K^+ (▼), 25%, 0.45 and 0.06 s^{-1}; chase with 1 mM K^+ (○), 25%, 1.0 and 0.09 s^{-1}; chase with 10 mM K^+ (▲), 25%, 1.5 and 0.13 s^{-1}. (B) Mutant Pro780→Ala: chase without added K^+ (□), 100%, 0.050 s^{-1} (single exponential); chase with 100 μM K^+ (▼), 25%, 0.2 and 0.001 s^{-1}; chase with 1 mM K^+ (○), 25%, 0.8 and 0.16 s^{-1}; chase with 10 mM K^+ (▲), 25%, 1.2 and 0.27 s^{-1}. (C) Mutant Leu332→Ala: chase without added K^+ (□), 100%, 0.033 s^{-1} (single exponential); chase with 100 μM K^+ (▼), 25%, 0.25 and 0.023 s^{-1}; chase with 1 mM K^+ (○), 25%, 0.49 and 0.054 s^{-1}; chase with 10 mM K^+ (▲), 25%, 0.68 and 0.056 s^{-1}. Right panels: The data were fitted to the modified Hill equation described under Materials and Methods. The respective values for $K_{0.5}(K^+)$ (indicated by dashed vertical lines in the figure) and the Hill coefficient, n, were (A) wild type, 97 μM, 1.0; (B) mutant Pro780→Ala, 601 μM, 1.1; (C) Leu332→Ala, 167 μM, 0.80.

wild type exhibited a $K_{0.5}$ for K^+ of 97 μM (Figure 4A, right panel), in good agreement with the $K_{0.5}$ value of 85 μM describing the K^+ concentration dependence of the steady-

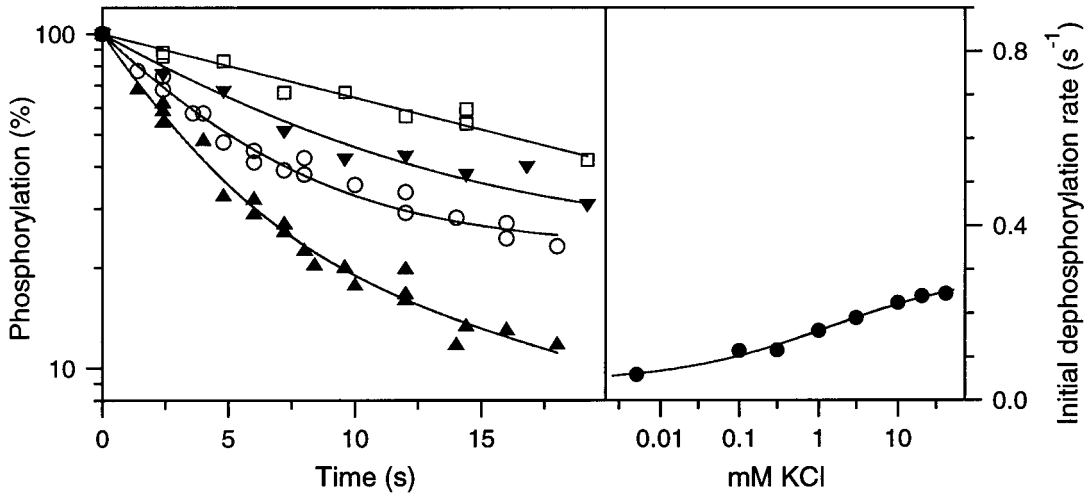

FIGURE 5: K^+-dependence of dephosphorylation of phosphoenzyme formed in presence of 2 mM NaCl in the mutant Gly330→Ala. Measurements and curve fitting were carried out as described for Figure 4. Left panel: Time courses of dephosphorylation at K^+-concentrations of 10 mM, 1 mM, 0.1 mM, and 5 μM (contaminant K^+). The respective values for the extent of the slow component of the decay curve and the rate coefficients of the fast and slow components were the following: chase without added K^+ (□), 100%, 0.044 s^{-1} (single exponential); chase with 100 μM K^+ (▼), 25%, 0.13 and 0.001 s^{-1}; chase with 1 mM K^+ (○), 25%, 0.22 and 0.004 s^{-1}; chase with 10 mM K^+ (▲), 25%, 0.32 and 0.046 s^{-1}. Right panel: Initial rates of dephosphorylation as a function of K^+ concentration (calculated from decays measured at 2.4 s, note the inclusion of data points corresponding to additional K^+ concentrations). The respective values for $K_{0.5}(K^+)$ and the Hill coefficient, *n*, were 1.43 mM and 0.44.

state phosphoenzyme level shown in Figure 1. Relative to the wild type, the apparent K^+ affinity displayed by the Pro780→Ala mutant (Figure 4B, right panel) was reduced about 6-fold ($K_{0.5}$ 601 μM). The respective rate coefficients of the rapid and the slow components in the K^+ dephosphorylation curve of mutant Pro780→Ala exhibited similar K^+ dependencies. However, the rate coefficient of the slow component displayed a 2-fold higher maximum value in the mutant relative to the wild type (for the individual rate coefficients of rapid and slow components, see legend to Figure 4).

The Leu332→Ala mutant exhibited a $K_{0.5}$ for K^+ of 167 μM, confirming the close to normal apparent affinity of this mutant for K^+ determined in the assays described above. It is of notice that the maximum initial rate of dephosphorylation of the Leu332→Ala mutant was reduced relative to that of the wild type (right panel of Figure 4) although the relative amount of E2P phosphoenzyme accumulated prior to dephosphorylation was approximately the same as in the wild type (60−70%, see Figure 2B). Extraction of the respective rate coefficients of the rapid and slow components showed a 2-fold reduction relative to the wild type for both components (legend to Figure 4, 10 mM K^+, compare the rate coefficients 0.68 and 0.056 s^{-1} corresponding to the mutant with 1.5 and 0.13 s^{-1} corresponding to the wild type).

In the light of the complex K^+ dependence of the steady-state phosphorylation level of mutant Gly330→Ala shown in Figure 1, it was considered worthwhile to make an attempt to determine the effect of K^+ on dephosphorylation of E2P in this mutant as well (Figure 5). The conditions were far from optimal since the amount of the E2P phosphoenzyme present prior to initiation of dephosphorylation constituted less than half that of the wild type (cf. Figure 2B), accounting for the rather slow dephosphorylation of the mutant. It was nevertheless clear that the Gly330→Ala mutant exhibited a more than 10-fold increase in $K_{0.5}$ for K^+ relative to the wild type and a Hill number well below 1 (Figure 5, right panel), suggesting that the two affinity components identified in the steady-state phosphorylation profile in Figure 1 may both be contributing to the K^+ effect on dephosphorylation.

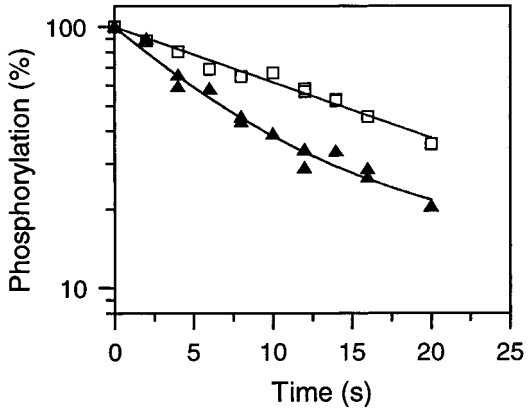

FIGURE 6: Effect of 20 mM K^+ on dephosphorylation of phosphoenzyme formed by the Leu332→Pro mutant in presence of 2 mM NaCl. Measurements and curve fitting were carried out as described for Figure 4. The respective values for the extent of the slow component of the decay curve and the rate coefficients of the fast and slow components were the following: chase without added K^+ (□), 100%, 0.049 s^{-1} (single exponential); chase with 20 mM K^+ (▲), 25%, 0.15 and 0.017 s^{-1}.

As seen in Figure 6, the effect of 20 mM K^+ on the rate of dephosphorylation of the phosphoenzyme formed by mutant Leu332→Pro at 2 mM Na^+ was minute, as might be expected because of the accumulation of the phosphoenzyme of this mutant in the K^+-insensitive E1P form (cf. Figure 2) and its slow conversion into K^+-sensitive E2P (cf. Figure 3). Decay curves obtained in similar experiments carried out at 130 mM Na^+ were indistinguishable from those shown in Figure 6. Moreover, when 20 mM K^+ was present from the beginning of the experiment during the phosphorylation, the decay curve was indistinguishable from that obtained by addition of K^+ with the ATP chase (results not shown). The rate coefficients determined by fitting the data obtained at 20 mM K^+ to the sum of two exponentials were lower than those determined at saturating K^+ concentration for any of the other mutants and the wild type. It is noteworthy that a

faster phosphoenzyme decay was observed at the same K^+ concentration following the salt jump (Figure 3), which may be ascribed to the increased free volume in the membrane lipid produced by movement of phase boundaries as a consequence of the sudden change in salt concentration. This is equivalent to the effect of a rise in temperature (*38*).

Effect of ATP and K^+ on the Dephosphorylation Kinetics of the Leu332→Ala Mutant in the Presence of EDTA

The observation in Figure 1 showing that in the Leu332→Ala mutant an unusual high level of phosphoenzyme was accumulated in the presence of K^+ is not straightforward to reconcile with the relatively rapid rates of K^+-induced dephosphorylation of this mutant depicted in Figure 3 (left panel) and Figure 4C (only 2-fold reduced relative to wild type). Because all the previously described dephosphorylation experiments had been carried out in the presence of 1 mM unlabeled ATP added to terminate phosphorylation from [γ-^{32}P]ATP, whereas the data in Figure 1 had been obtained in the presence of 2 μM ATP, the question arose whether the high ATP concentration in any way might affect the rate of dephosphorylation of mutant Leu332→Ala. Hence, a series of dephosphorylation experiments was conducted in which EDTA instead of unlabeled ATP was used to terminate phosphorylation (by chelating catalytic Mg^{2+}), so that the concentration of ATP could be kept low corresponding to the 2 μM added initially to phosphorylate the enzyme. Interestingly, as seen in Figure 7 at this low ATP concentration (i.e., conditions similar to those of Figure 1) the rate of K^+-induced dephosphorylation of the Leu332→Ala mutant was 4−5-fold reduced relative to that of the wild type, explaining the difference between wild type and mutant with respect to steady-state phosphoenzyme accumulation in the presence of K^+ shown in Figure 1. The mutant dephosphorylated slowly irrespective of whether K^+ was present from the start during phosphorylation or was added together with EDTA during chase of the phosphoenzyme (Figure 7A, compare filled and open circles). A more rapid phosphoenzyme decay almost identical to that of Figure 4C (maximum K^+ concentration) was observed for the mutant when ATP at a concentration of 100 μM or 1 mM was included in the dephosphorylation medium in addition to EDTA and K^+ (Figure 7A, diamonds). This behavior differs from that of the wild type, for which the rate of K^+-induced dephosphorylation was insensitive to an increase in ATP concentration from 2 μM to 1 mM (Figure 7B, compare open circles and diamonds), in accordance with the literature (*40*, *41*).

In the absence of K^+, addition of ADP with EDTA resulted in decay curves similar to those obtained by addition of ADP with ATP (compare Figures 2B and 7), extrapolating back to ordinate intercept at 60−70% E2P for the Leu332→Ala mutant as well as the wild type. When in addition to ADP and EDTA K^+ was included, the phosphoenzyme decay of the Leu332→Ala mutant became monophasic and rapid, resembling that observed with mutant Leu332→Pro (Figure 7A, open and filled triangles pointing upward, compare with filled squares). It is of notice, that more than 90% of the phosphoenzyme disappeared during 2 s of dephosphorylation in the simultaneous presence of K^+ and ADP, whereas the sum of the separate effects of K^+ (Figure 7A, circles) and ADP (Figure 7A, open triangles pointing downward) amounted to maximally 70%, even though in this sum phosphoenzyme

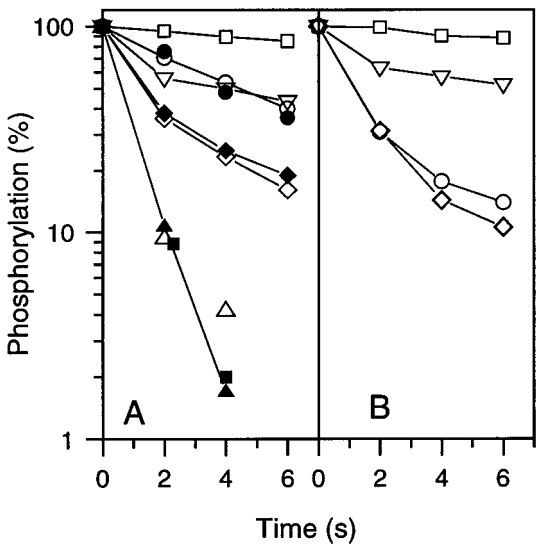

FIGURE 7: K^+-, ADP-, and ATP-dependencies of dephosphorylation following termination of phosphorylation with EDTA in mutant Leu332→Ala (A) and the wild-type Na^+,K^+-ATPase (B). Phosphorylation was carried out in 100 μL of standard medium in the presence of 20 mM NaCl with or without 20 mM KCl, and terminated by the addition of 10 μL of a chase solution (corresponding to zero time) producing a final concentration of 10 mM EDTA. During dephosphorylation, the final concentrations of K^+, ADP, and ATP (varied by adjusting the concentrations in the chase solution) were as follows: (□) no other components; (○) 20 mM KCl (added with chase solution); (●) 20 mM KCl (present from start of phosphorylation); (▽) 2.5 mM ADP (added with chase solution); (◇) 20 mM KCl and 1 mM ATP (both components added with chase solution); (◆) 20 mM KCl and 100 μM ATP (both components added with chase solution); (△) 20 mM KCl and 2.5 mM ADP (both components added with chase solution); (▲) 20 mM KCl (present from start of phosphorylation) and 2.5 mM ADP (added with chase solution). In panel A, the above described symbols represent mutant Leu332→Ala, but in addition a single experiment with mutant Leu332→Pro is shown (■) corresponding to dephosphorylation in the presence of 20 mM KCl (present from start of phosphorylation) and 2.5 mM ADP (added with chase solution). In panel B, all data correspond to the wild type.

sensitive to both ADP and K^+ is counted twice (*35*, *36*). A possible explanation is that in the Leu332→Ala mutant, K^+ is able to drive the interconversion of E1P to E2P backward, forming ADP-sensitive phosphoenzyme, which is rapidly dephosphorylated in the simultaneous presence of ADP.

DISCUSSION

This report describes for the first time point mutations in the Na^+,K^+-ATPase that affect the ion-translocating E1P to E2P conformational change of the phosphoenzyme.

Mutants Leu332→Pro and Gly330→Ala exhibited a similar behavior in many respects. Under conditions where a high level of the ADP-insensitive and K^+-sensitive E2P phosphoenzyme accumulated in the wild-type Na^+,K^+-ATPase (low Na^+ concentration and absence of K^+), the phosphoenzyme intermediate formed by the mutants Leu332→Pro and Gly330→Ala resided predominantly in the ADP-sensitive E1P form, as indicated by the dephosphorylation kinetics measured in the presence of ADP at 0 °C as well as by the ADP−ATP exchange activity measured at 26 °C. During turnover in the presence of a K^+ concentration where the wild type resides predominantly in an unphosphorylated state, these two mutants exhibited a high steady-state phosphoenzyme level and a high ADP−ATP exchange

activity. Furthermore, following phosphorylation in the presence of 600 mM Na^+ to ensure accumulation of E1P even in the wild type, the phosphoenzymes of the two mutants Leu332→Pro and Gly330→Ala decayed slowly relative to the wild-type phosphoenzyme when K^+ was added to dephosphorylate E2P simultaneously with a downward jump in salt concentration to induce conversion of E1P to E2P (Figure 3, left panel). Under these circumstances, the decay curves of mutants Leu332→Pro and Gly330→Ala resembled that obtained with the wild-type enzyme when the Na^+ concentration was maintained at a high value (Figure 3, right panel). Taken together, these data clearly demonstrate that in the mutants Leu332→Pro and Gly330→Ala the E1P to E2P transition was slowed down relative to the corresponding transition in the wild type. The most dramatic effects were observed for the Leu332→Pro mutation. Hence, the amount of E2P accumulated at steady state, the rate coefficients associated with decay of E1P in the presence of K^+, and the maximum turnover number for the overall enzyme cycle were all found to be lower in the Leu332→Pro mutant compared with the Gly330→Ala mutant.

One may ask how the reduction of the rate of the E1P to E2P interconversion of the Leu332→Pro mutant compares to the reduction in the rate of the overall reaction cycle? In this mutant, the rate coefficients of the two kinetic components of the E1P decay observed following the salt jump were each reduced by at least a factor of 2 relative to the corresponding values for the wild type, and there was an increase in the extent of the slow component from 7% in the wild type to 48% in the mutant (Figure 3, left panel), which would correspond to a more pronounced reduction in the rate of the E1P to E2P transition compared with the rate of the overall reaction (the turnover rate of the mutant was 64% that of the wild type, cf. Table 1). At least two circumstances may contribute to this. First, it should be taken into consideration that for technical reasons the measurements of the rate of the overall reaction cycle and of the E1P decay were conducted at widely different temperatures (37 and 0 °C, respectively). Second, the E1P to E2P interconversion is not likely to constitute the only or major rate-determining step in the reaction cycle of the wild type (note that for the wild-type Na^+,K^+-ATPase Klodos et al. (*39*) found a rate coefficient of 60 s^{-1} for the E1P to E2P transition at 20 °C, whereas the turnover rate for the overall reaction cycle was about 20 s^{-1} at the same temperature). Therefore, the decrease in the rate of the E1P to E2P transition induced by the mutation is not expected to be fully reflected in the rate of the overall reaction.

A most remarkable feature of the phosphoenzyme formed by the Leu332→Pro mutant is its manifest insensitivity to K^+ at 0 °C. In the presence of 60 mM K^+, the steady-state phosphoenzyme level of the mutant amounted to as much as 90% of the maximum level determined in the absence of K^+, whereas the phosphoenzyme level of the wild type was reduced to 20% under these conditions (Figure 1). Since the apparent affinity for K^+ determined for mutant Leu332→Pro was wild-type like in the ATPase assay at 37 °C, the K^+ insensitivity at 0 °C must be ascribed to the low rate of the E1P to E2P conversion under the latter conditions, in accordance with the concept that only E2P is dephosphorylated by K^+ (*7*). Computer simulations of the enzyme cycle based on the Albers−Post model show that variations in the height of the plateau phosphorylation level such as seen in Figure 1 can be reproduced by changing the rate coefficients associated with the interconversion of the phosphoenzyme intermediates E1P and E2P. The plateau level rises if the rate coefficient of the forward transformation of E1P to E2P is reduced or that of the reverse reaction increased.

The Leu332→Pro and Gly330→Ala mutants furthermore displayed higher apparent Na^+ and ATP affinities than the wild type (Table 1). This may possibly indicate that the mutations poised the E1−E2 equilibrium of the dephosphoenzyme in favor of the E1 form possessing high affinity for Na^+ and ATP, in parallel with the stabilization of the phosphoenzyme in the E1P form. A contributing factor might also be the reduced E1P to E2P transition rate in the mutants, which at nonsaturating Na^+ and ATP concentrations should lead to accumulation of more phosphoenzyme in the mutants relative to the wild type, and thus to an increase in apparent affinity for Na^+ and ATP. Such an effect can indeed be demonstrated by computer simulation of the enzyme cycle according to the Albers−Post model. It is noteworthy, however, that the increase in Na^+ affinity measured in the phosphorylation assay amounted to as much as 5-fold in the Gly330→Ala mutant, whereas it was less (1.5-fold) in the Leu332→Pro mutant (Table 1), although as discussed above the latter mutant showed the most pronounced block of the E1P to E2P conversion. In addition, the Gly330→Ala mutant displayed a conspicuous reduction of the apparent K^+ affinity determined in the phosphorylation and dephosphorylation assays as well as by K^+ titration of the Na^+,K^+-ATPase activity (Figures 1 and 5, Table 1). Gly330 is located right next to the glutamic acid residue Glu329 suggested to contribute its side chain oxygen atoms to the coordination spheres of the cations and/or to be part of a gate at the cytoplasmic entrance to the cation binding pocket (*2*, *3*, *21*, *22*), and Gly330 may be an important structural element determining the conformational properties locally in the cation binding pocket. K^+ titration of the phosphoenzyme of the Gly330→Ala mutant provided evidence for two affinity components (Figure 1 and Figure 5, right panel). This could be due to the existence of two phosphoenzyme pools differing in their K^+ dependence of dephosphorylation. Alternatively, one of two K^+ sites on the same enzyme molecule may have been more seriously affected by the mutation than the other (assuming that each site contributes separately to control of the dephosphorylation rate), or the cooperative interaction between the sites may have been disturbed along with the perturbation of the E1P to E2P transition.

In the most simple version of the Albers−Post model (*7*, *8*), dephosphorylation of E1P in the presence of K^+ occurs through the conversion of K^+-insensitive E1P to K^+-sensitive E2P and subsequent K^+-induced hydrolysis of the latter intermediate. It was only possible to fit the time dependence of K^+-induced dephosphorylation in mutants as well as wild type (Figures 4 and 5) to the sum of two exponentials if both rate coefficients were allowed to increase with increasing K^+ concentration, in apparent contradiction with the hypothesis that only one phosphoenzyme pool (E2P) reacts with K^+. Two components were likewise observed in the decays of the E1P phosphoenzyme intermediate of mutants Leu332→Pro and Gly330→Ala following the salt jump (Figure 3). Moreover, for these mutants the ADP-sensitive phosphoenzyme determined by the analysis shown in Figure

2 amounted to 100% and 72%, respectively, at 2 mM Na^+, whereas the extent of the slow component in the corresponding K^+-dephosphorylation curves (Figures 5 and 6) constituted only around 25%, suggesting that part of the phosphoenzyme is sensitive to both ADP and K^+. Related phenomena have been observed previously with the wild type under various conditions and are extensively discussed in several papers (see for instance (*35*−*39*, *42*−*44*)). One source of complexity is the possible existence of phosphoenzyme species interposed between E1P and E2P in the reaction path. Such intermediate forms ("E*P") might be sensitive to both ADP and K^+ or might be rapidly interconvertible with either of the two "classic intermediates". Moreover, one has to consider that both the ADP-sensitive and the K^+-sensitive phosphoenzyme pools may be kinetically heterogeneous due to heterogeneity of the lipid environment or of oligomerization state of the Na^+,K^+-ATPase protomers (*38*, *44*). Although in the present study no attempt was made to resolve the decay curves into more than the classic two components, this would clearly be feasible. Because the present data were obtained with a system in which the expressed ouabain-resistant rat α_1-isoform was the only functioning Na^+,K^+-ATPase, the coexistence of various isozymes as a possible source of heterogeneous kinetics can be excluded.

For mutant Pro780→Ala as for the wild type, the prevailing phosphoenzyme intermediate at low Na^+ concentration and absence of K^+ was the ADP-insensitive and K^+-sensitive E2P form. Under these conditions, studies of K^+ dependence of dephosphorylation as presented in Figure 4 may provide a relatively accurate measure of the affinity for K^+ at the extracellularly facing sites. Using this method the apparent affinity for K^+ of mutant Pro780→Ala was found to be reduced approximately 6-fold relative to that of the wild-type Na^+,K^+-ATPase, which compares favorably with the 5-fold reduction determined in the assay for Na^+,K^+-ATPase activity (Table 1) and in the K^+ titration of the steady-state phosphorylation level (Figure 1). The reduced K^+ affinity as well as the 2-fold increase in the maximum value of the rate coefficient of the slow decay component of E2P displayed by mutant Pro780→Ala would be consistent with a role for the proline in optimizing the position of the side chain of the adjacent glutamic acid residue Glu781 thought to be involved in the discrimination between extracellular Na^+ and K^+ and/or in the signal transmission leading to dephosphorylation of E2P (*4*, *45*). It is noteworthy that the Na^+ affinity determined in the ATPase and phosphorylation assays was normal in the Pro780→Ala mutant. Hence, the proline is not important for the function of the cytoplasmically facing Na^+ sites in the E1 form.

The mutant Leu332→Ala, like mutant Leu332→Pro, displayed a highly significant reduction in the maximum turnover rate and a high steady-state level of phosphoenzyme even at high K^+ concentrations (Figure 1). However, the mechanism behind these changes in overall function relative to the wild type seems to be different from that pertaining to the Leu332→Pro mutant. In the Leu332→Ala mutant, a high level of ADP-insensitive phosphoenzyme accumulated in the absence of K^+, and no ADP−ATP exchange activity was detected at low Na^+ concentration without K^+. K^+ induced rapid dephosphorylation when added together with ADP but not when added separately at low ATP concentration (Figure 7). Hence, at low ATP concentration, the sum of the K^+- and ADP-induced dephosphorylations was less than the dephosphorylation observed in the simultaneous presence of K^+ and ADP, whereas the opposite might have been expected because of overlap between ADP-sensitive and K^+-sensitive phosphoenzyme pools (*35*, *36*). In combination with the finding that the ADP−ATP exchange activity rised sharply in the presence of K^+ (Table 2), these data seem to indicate that in mutant Leu332→Ala K^+ induced reversal of the phosphoenzyme interconversion forming ADP-sensitive E1P from E2P. At low ATP concentration in the absence of added ADP, the K^+-dependent dephosphorylation of preaccumulated E2P seemed to occur with a 4−5-fold lower rate in the mutant relative to the wild type (Figure 7), and in the presence of 1 mM ATP the rate was still about 2-fold lower in the mutant relative to the wild type (Figures 4 and 7). Because the apparent K^+ affinity determined for mutant Leu332→Ala in the K^+ titrations of Na^+,K^+-ATPase activity and dephosphorylation rate was similar to that of the wild type, there was probably little effect of the mutation on the K^+ binding properties of the enzyme. It is therefore conceivable that the mechanism underlying the reduced dephosphorylation rate is the depletion of K^+-sensitive E2P being converted back to nonproductive E1P upon K^+ binding.

An important consideration in relation to the enhancement of the rate of K^+-induced dephosphorylation of mutant Leu332→Ala observed upon increasing the ATP concentration from 2 μM to 1 mM (Figures 4 and 7) is whether the phosphoenzyme decay occurred at least partly through back conversion of E2P to E1P and dephosphorylation of E1P by contaminant ADP. Against this interpretation stands the fact that the added ATP had been purified to contain less than 0.2% ADP (see Materials and Methods) and that the response was unaltered following a 10-fold dilution of the added ATP (Figure 7A), which also diluted contaminant ADP. Moreover, contaminant ADP present in amounts causing dephosphorylation of the Leu332→Ala mutant would be expected to dephosphorylate the E1P intermediate accumulated in mutant Leu332→Pro at high Na^+ concentration as well, but this intermediate did not respond to the ATP chase (Figure 3, right panel).

Another possibility is that the added ATP acts as modulator, enhancing the rate of E2P dephosphorylation and/or preventing E2P from being back converted into nonproductive E1P in the Leu332→Ala mutant. For the wild-type Na^+,K^+-ATPase, there is no firm evidence of a modulatory effect of ATP on the kinetic properties of the phosphoenzyme (*40*, *41*), but in the closely related Ca^{2+}-ATPase of sarcoplasmic reticulum the rate of E2P dephosphorylation is enhanced at least 2-fold by ATP in the concentration range studied here (*46*, *47*). The modulatory ATP site in the Ca^{2+}-ATPase (possibly identical to the catalytic site) seems to exhibit higher affinity in E2P relative to E1P (*46*−*48*). A similar difference between the E1P and E2P forms of Na^+,K^+-ATPase with respect to ATP affinity would imply that ATP stabilizes E2P relative to E1P, thereby counteracting the back conversion of E2P into E1P in the mutant.

The present data suggest that the PEGLL332 segment of the Na^+,K^+-ATPase, possibly with adjoining residues, plays a pivotal role in the conformational changes of the phosphoenzyme associated with ion translocation. The central role for this peptide segment in the mediation of long-range coupling between the catalytic site and the cation binding

sites in the membrane domain is consistent with the location at the cytoplasmically facing end of the putative transmembrane α-helix M4, linking M4 physically to the part of the cytoplasmic domain containing the phosphorylated aspartyl residue. As discussed above, replacement of Leu332 in Na^+,K^+-ATPase with proline and alanine affected the functional characteristics of the phosphoenzyme in separate ways. In general, proline residues possess unique structural and functional properties (*49*). It is possible that the substitution of proline for leucine at position 332 sterically hindered the E1P to E2P conformational transition by introducing a kink in the M4 helix. The finding that the inverse Pro312→Leu substitution at the homologous position in the Ca^{2+}-ATPase likewise inhibited the E1P to E2P transformation of this enzyme (*15*) demonstrates that a normal progression of the E1P to E2P transformation requires specific interaction between the leucine/proline and matching peptide structures that cannot be provided by the other related ATPase. The enhancement of the back conversion of E2P to E1P by replacement of the bulky aliphatic side chain of Leu332 in Na^+,K^+-ATPase with the smaller alanine side chain may be attributable to a weakening of hydrophobic interactions between M4 and other transmembrane segments in E2P.

ACKNOWLEDGMENT

I thank Dr. Jens Peter Andersen for many helpful discussions and suggestions, Janne Petersen, Jytte Jørgensen, and Lene Jacobsen for their expert and invaluable technical assistance, and Dr. R. J. Kaufman, Genetics Institute, Boston, MA, for the gift of the expression vector pMT2.

REFERENCES

1. Glynn, I. M. (1993) *J. Physiol. 462*, 1−30.
2. Lingrel, J. B., and Kuntzweiler, T. (1994) *J. Biol. Chem. 269*, 19659−19662.
3. Andersen, J. P., and Vilsen, B. (1995) *FEBS Lett. 359*, 101−106.
4. Vilsen, B. (1995) *Biochemistry 34*, 1455−1463.
5. Lutsenko, S., and Kaplan, J. H. (1995) *Biochemistry 34*, 15607−15613.
6. Kuntzweiler, T. A., Argüello, J. M., and Lingrel, J. B. (1996) *J. Biol. Chem. 271*, 29682−29687.
7. Post, R. L., Kume, S., Tobin, T., Orcutt, B., and Sen, A. K. (1969) *J. Gen. Physiol. 54*, 306s−326s.
8. Post, R. L., Hegyvary, C., and Kume, S. (1972) *J. Biol. Chem. 247*, 6530−6540.
9. Beaugé, L. A., and Glynn, I. M. (1979) *J. Physiol. 289*, 17−31.
10. Glynn, I. M., Hara, Y., and Richards, D. E. (1984) *J. Physiol. 351*, 531−547.
11. Jørgensen, P. L., Klodos, I., and Petersen, J. (1978) *Biochim. Biophys. Acta 507*, 8−16.
12. Jørgensen, P. L., and Petersen J. (1985) *Biochim. Biophys. Acta 821*, 319−333.
13. Steinberg, M., and Karlish, S. J. D. (1989) *J. Biol. Chem. 264*, 2726−2734.
14. Taniguchi, K., Tosa, H., Suzuki, K., and Kamo, Y. (1988) *J. Biol. Chem.* 263, 12943−12947.
15. Vilsen, B., Andersen, J. P., Clarke, D. M., and MacLennan, D. H. (1989) *J. Biol. Chem. 264*, 21024−21030.
16. Vilsen, B., Andersen, J. P., and MacLennan, D. H. (1991) *J. Biol. Chem. 266*, 18839−18845.
17. Inesi, G., Chen, L., Sumbilla, C., Lewis, D., and Kirtley, M. E. (1995) *Biosci. Rep. 15*, 327−339.
18. Garnett, C., Sumbilla, C., Belda, F. F., Chen, L., and Inesi, G. (1996) *Biochemistry 35*, 11019−11025.
19. Vilsen, B. (1992) *FEBS Lett. 314*, 301−307.
20. Vilsen, B. (1993) *Biochemistry 32*, 13340−13349.
21. Kuntzweiler, T. A., Wallick, E. T., Johnson, C. L., and Lingrel, J. B. (1995) *J. Biol. Chem. 270*, 2993−3000.
22. Vilsen, B. (1995) *Acta Physiol. Scand. 154* (Suppl. 624), 1−146.
23. Andersen, J. P., Vilsen, B., and MacLennan, D. H. (1992) *J. Biol. Chem. 267*, 2767−2774.
24. Kunkel, T. A. (1985) *Proc. Natl. Acad. Sci. U.S.A. 85*, 3314−3318.
25. Sanger, F., Nicklen, S., and Coulson, A. R. (1977) *Proc. Natl. Acad. Sci. U.S.A. 74*, 5463−5467.
26. Kaufman, R. J., Davies, M. V., Pathak, V. K., and Hershey, J. W. B. (1989) *Mol. Cell. Biol. 9*, 946−958.
27. Gluzman, Y. (1981) *Cell 23*, 175−182.
28. Bradford, M. M. (1976) *Anal. Biochem. 72*, 248−254.
29. Fahn, S., Koval, G. J., and Albers, W. (1966) *J. Biol. Chem. 241*, 1882−1889.
30. Randerath, K., and Randerath, E. (1967) *Methods Enzymol. 12*, 323−347.
31. Yu, X., and Inesi, G. (1995) *J. Biol. Chem. 270*, 4361−4367.
32. Palasis, M., Kuntzweiler, T. A., Argüello M. J., and Lingrel, J. B. (1996) *J. Biol. Chem. 271*, 14176−14182.
33. Esmann, M. (1988) *Methods Enzymol. 156*, 105−115.
34. Han, C. S., Tobin, T., Akera, T., and Brody, T. M. (1976) *Biochim. Biophys. Acta 429*, 993−1005.
35. Nørby, J. G., Klodos, I., and Christiansen, N. O. (1983) *J. Gen. Physiol. 82*, 725−759.
36. Yoda, S., and Yoda, A. (1986) *J. Biol. Chem. 261*, 1147−1152.
37. Nørby, J. G., and Klodos, I. (1988) in *The Na^+,K^+-Pump, Part A: Molecular Aspects* (Skou, J. C., Nørby, J. G., Maunsbach, A. B., and Esmann, M., Eds.) pp 249−270, Alan R. Liss, Inc., New York.
38. Post, R. L., and Klodos, I. (1996) *Am. J. Physiol. 271*, C1415-C1423.
39. Klodos, I., Post, R. L., and Forbush, B., III (1994) *J. Biol. Chem. 269*, 1734−1743.
40. Hobbs, A. S., Albers, R. W., Froehlich, J. P., and Heller, P. F. (1985) *J. Biol. Chem. 260*, 2035−2037.
41. Klodos, I., and Nørby, J. G. (1988) in *The Na^+,K^+-Pump, Part A: Molecular Aspects* (Skou, J. C., Nørby, J. G., Maunsbach, A. B., and Esmann, M., Eds.) pp 321−326, Alan R. Liss, Inc., New York.
42. Glynn, I. M. (1988) in *The Na^+,K^+-Pump Part A: Molecular Aspects* (Skou, J. C., Nørby, J. G., Maunsbach, A. B., and Esmann, M., Eds.) pp 435−460, Alan R. Liss, Inc., New York.
43. Froehlich, J. P., and Fendler, K. (1991) in *The Sodium Pump: Structure, Mechanism, and Regulation* (Kaplan, J. H., and De Weer, P., Eds.) Vol. 46, pp 227−247, Society General Physiologists Series 46, Rockefeller University Press, New York.
44. Martin, D. W., and Sachs, J. R. (1991) *J. Gen. Physiol. 98*, 419−426.
45. Koster, J. C., Blanco, G., Mills, P. B., and Mercer, R. W. (1996) *J. Biol. Chem. 271*, 2413−2421.
46. Champeil, P., Riollet, S., Orlowski, S., Guillain, F., Seebregts, C. J., and McIntosh, D. B. (1988) *J. Biol. Chem. 263*, 12288−12294.
47. Lund, S., and Møller, J. V. (1988) *J. Biol. Chem. 263*, 1654−1664.
48. Vilsen, B., and Andersen, J. P. (1987) *Eur. J. Biochem. 170*, 421−429.
49. Williams, K. A., and Deber, C. M. (1991) *Biochemistry 30*, 8919−8923.

BI971030Q